SAÜ Fen Bil Der 20. Cilt, 3. Sayı, s. 543-558, 2016

ACACETIN'İN (5,7-dihydroxy-4'-methoxyflavone) moleküler yapisinda titreşimsel spektral analizler ve teorik inceleme

Tevfik Raci Sertbakan[1*], Ökkeş Gözdaş[2]

29.03.2016 Geliş/Received, 01.08.2016 Kabul/Accepted

doi: 10.16984/saufenbilder.67441

ÖZ

Bitkilerde doğal olarak mevcut bir flavon bileşiğiolan Acacetin (5,7-dihydroxy-4'-methoxyflavone) anti-kanser ve anti-iltihap aktivitelere sahiptir. Nöroiltihabın Parkinson hastaları (PD) için güvenilir başlıca patolojik meknizmalardan biri olduğu düşünülmektedir ve PD için tedavi gelişiminde bir ana hedef olmuştur. Bu çalışmada, acacetinin molekülünün konformasyon araştırması yapılmıştır. Bu bileşiğin FT-IR spektrumu 4000–400 cm^{-1} bölgesinde kaydedilmiştir. FT-Raman spektrumu da 3500–50 cm^{-1} bölgesinde kaydedilmiştir. Başlık bileşiğinin titreşim frekansları B3LYP metodu cc-pVDZ ve cc-pVTZ temel setlerinde hesaplanmıştır. Bu hesaplamalar, gradyent geometri optimizasyonu yardımıyla Gaussian 09W paket programı kullanılarak DFT seviyelerinde gerçekleşmiştir. Titreşim frekanslarının ve geometrik parametrelerin hesaplamaları analiz edilmiş ve deneysel sonuçlar ile karşılaştırılmıştır.

Anahtar Kelimeler: Acacetin, flavon, FT-IR, FT-Raman, Yoğunluk fonksiyonu teorisi, Toplam enerji dağılımı

Vibrational spectral analysis and theoretical ınvestıgatıon on the molecular structure of ACACETIN (5,7-dihydroxy-4'-methoxyflavone)

ABSTRACT

Acacetin (5,7-dihydroxy-4'-methoxyflavone) which is naturally a flavone compounds presents in plants, has anti-cancer and anti-inflammatory activities. Neuroinflammation is thought to be one of the major pathological mechanisms responsible for Parkinson's disease (PD), and has been a primary target in the development of treatment for PD. In this study, conformational search of the acacetin molecule has been performed. The FT-IR spectrum of this compound was recorded in the region 4000–400 cm^{-1}. The FT-Raman spectrum was also recorded in the region 3500–50 cm^{-1}. Vibrational frequencies of the title compound have been calculated by B3LYP with cc-pVDZ and cc-pVTZ basis sets. The calculations were performed at DFT levels by using Gaussian 09W program package, by invoking gradient geometry optimization. The calculated geometric parameters and vibrational frequencies were analyzed and compared with obtained experimental results.

Keywords: Acacetin, Flavone, FT-IR, FT-Raman, Density functional theory, Total energy distribution

[*] Sorumlu Yazar / Corresponding Author
[1] Ahi Evran Üniversitesi, Fen Edebiyat Fakültesi, Fizik Bölümü, KIRŞEHİR - trsertbakan@ahievran.edu.tr
[2] Ahi Evran Üniversitesi, Fen Edebiyat Fakültesi, Fizik Bölümü, KIRŞEHİR - ogozdas@gmail.com

1. INTRODUCTION

Flavonoids are known large group of naturally occurring compounds in plants [1]. They have many various applications and properties [1]. Flavonoids are responsible for many phenomena such as the shades of yellow, orange and red in flowering plants, and important factors for plant growth, development and protection [1].

Flavonoids relate to a large family of natural polyphenolic compounds that are ordinarily found in the human diet particularly in fruits, vegetables and beverages such as tea and red wine [2]. These compounds display a kind of pharmacological properties in the therapy of several diseases, including cancer, as cytotoxic, antiangiogenic, or antivascularagents [2].

Acacetin (5,7-dihydroxy-4'-methoxyflavone) molecule ($C_{16}H_{12}O_5$) is one of the flavonoid compounds. It has anticancer, anti-inflammatory and anti-peroxidative effect [3]. Acacetin, a constituent of flavone naturally present in plants, has anti-cancer and anti-inflammatory activities. Neuroinflammation is thought to be one of the major pathological mechanisms responsible for Parkinson's disease (PD), and has been a primary target in the development of treatment for PD [4].

Flavone has been examined by Raman and surface-enhanced Raman spectra [5], Gas phase infrared spectra [6]. It was realized ab initio conformational analysis of flavone and related compounds [7]. Vibrational frequency of flavone and some deuterated analogues have been calculated from the conformational analysis of flavone using the semi-empirical AM1 method and compared with experimental values [8]. These calculations were used in united molecular mechanics, semi-empirical and ab initio calculations. Although semi-empirical methods attested its benefits in application to facilitate the IR definitions, the performance of semi-empirical methods can not satisfy modern criteria of theoretical FT-IR spectral predictions. The infrared spectra were calculated with density functional theory (DFT) methods were in much better agreement with the observed infrared spectrum. The calculated band intensities is jibed with the observed relative intensities as well [9].
In this study, we reported theoretical calculations of molecular structure and vibrational spectra of acacetin (5,7-dihydroxy-4′-methoxyflavone) molecule. We are now reporting the results of calculation and experimental (IR and Raman) spectra of the acacetin molecule in density functional theory (DFT) approximations. The present investigation was undertaken to study the vibrational spectra of this molecule completely and to define the diverse modes with larger wavenumber certainty. Density functional theory (DFT) calculations have been performed to support our wavenumber assignments. Furthermore, we interpreted the calculated spectra in terms of total energy distributions (TED's) and made the assignment of the experimental bands based on TED analysis results.

2. EXPERIMENTAL

Acacetin molecule was purchased from Sigma–Aldrich Chemical Company. IR spectrum of acacetin molecule at room temperature was recorded by using a Perkin Elmer Spectrum One FT–IR spectrometer in the region 400–4000 cm^{-1} with a resolution of 2 cm^{-1}. The sample was compressed into self-supporting pellet and introduced into an IR cell equipped with KBr window. Also, the Raman spectrum of acacetin molecule was recorded with a JascoNRS-3100 micro-Raman Spectrophotometer (1200 lines/mm grating and high sensitive cooled CCD) at room temperature in the region 50–4000 cm^{-1}. The sample was stimulated by using 785 nm diode laser. The spectrometer was calibrated with the silicon phonon mode at 520 cm^{-1} and microscope objective 100 was used. The measured and calculated FT-IR and micro-Raman spectra are shown in Fig. 1 a, b, c and Fig. 2 a, b, c.

3. COMPUTATIONAL DETAILS

The structure of acacetin in the primary level is optimized by B3LYP method with cc-pVDZ basis set. Vibrational frequencies of the title compound have been calculated by DFT (B3LYP –cc-pVDZ and cc-pVTZ basis sets) approximations and then scaled by corresponding scaling factor. The calculations were performed at DFT levels by using Gaussian 09W program package, invoking gradient geometry optimization [10,11]. The calculated geometric parameters and vibrational frequencies were analyzed and compared with obtained experimental results.

4. RESULT AND DISCUSSION

4.1. Conformational Stability

The diverse conformational structures of a compound are correlated with many of the physical and chemical properties. Hence, their investigation is important for drug designs and to understand several medicinal effects [12]. The conformational analysis was realized for the acacetin molecule. The geometry optimizations of the obtained conformers were performed by B3LYP/cc-pVDZ level of theory. Results of conformational analysis showed that acacetin molecule has twelve conformers as shown in Fig. 3.

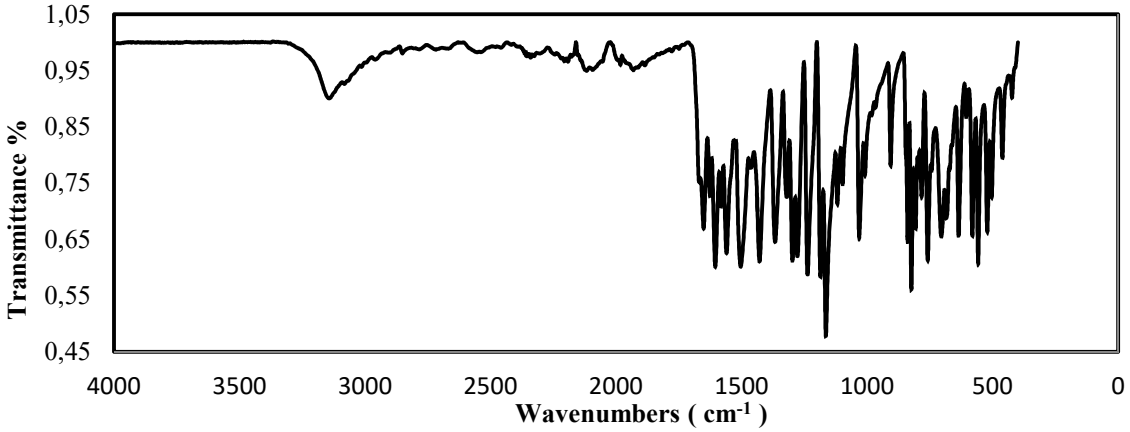

a – Experimental IR spectra of acacetin molecule.

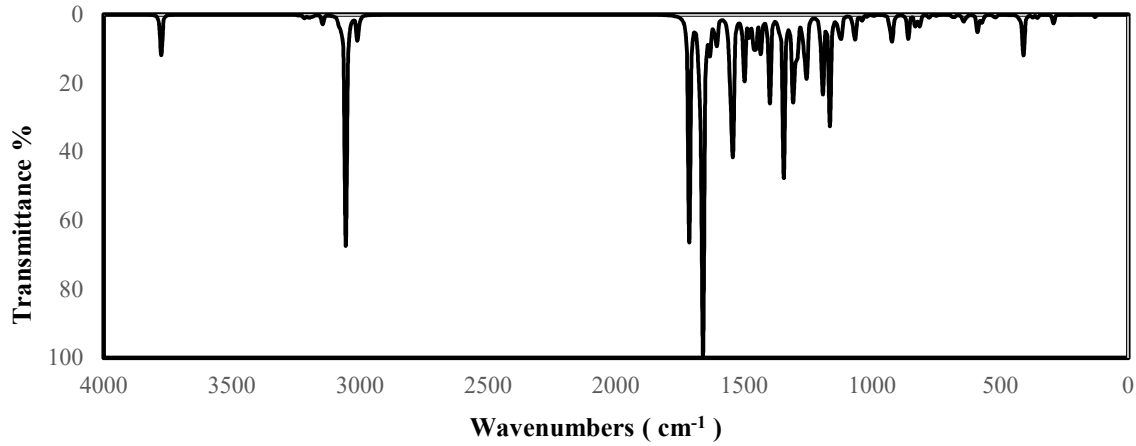

b – Theoretical (with cc-pVDZ basis set) IR spectra of acacetin molecule.

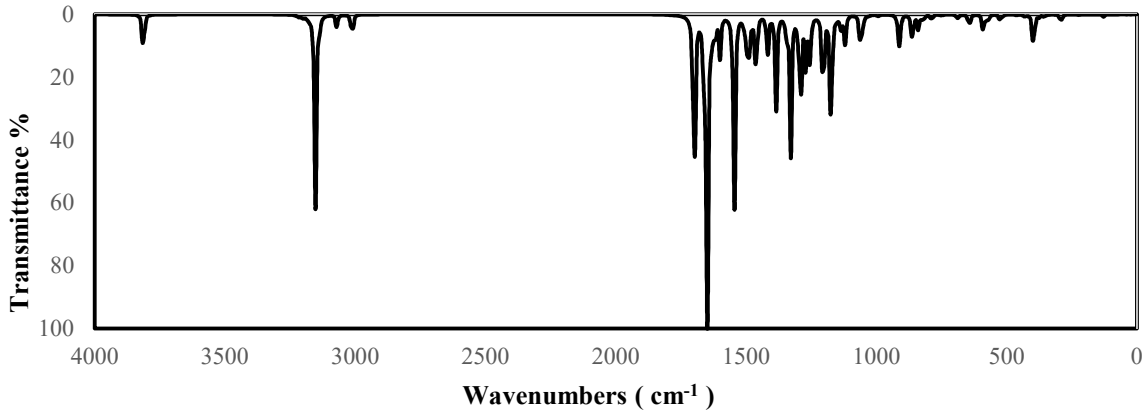

c – Theoretical (with cc-pVTZ basis set) IR spectra of acacetin molecule.

Fig. 2 Experimental and theoretical IR spectra of acacetin molecule.

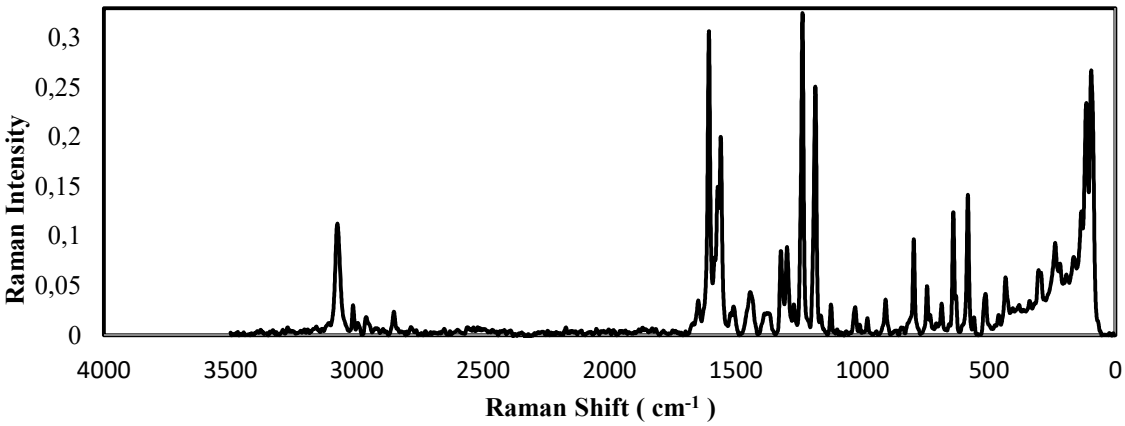

a – Experimental Raman spectra of acacetin molecule.

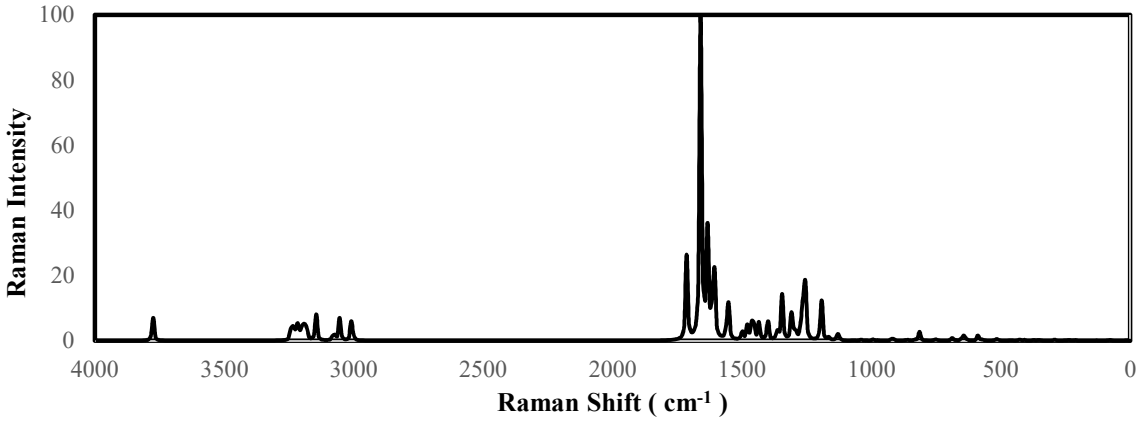

b – Theoretical (with cc-pVDZ basis set) Raman spectra of acacetin molecule.

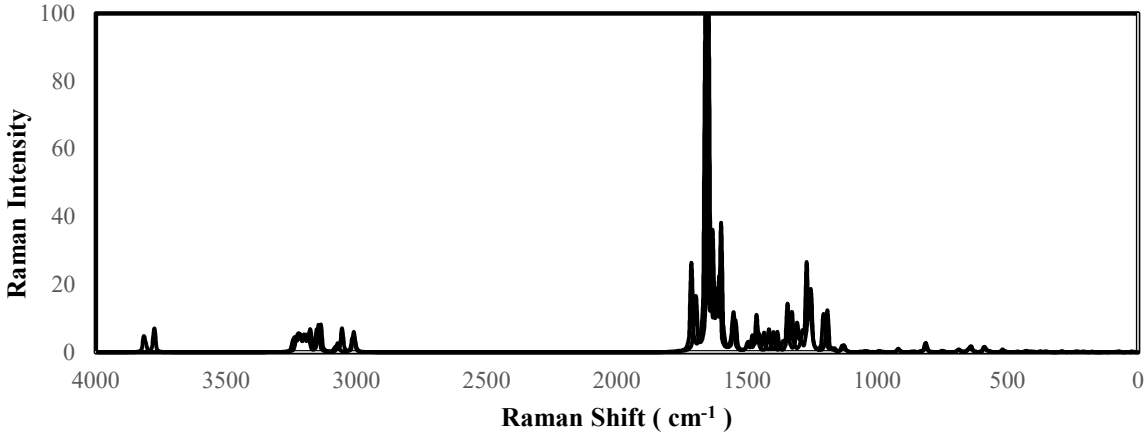

c – Theoretical (with cc-pVTZ basis set) Raman spectra of acacetin molecule.

Fig. 2 Experimental and theoretical Raman spectra of acacetin molecule.

Table.1 The calculated energies of twelve conformers, given in

Conformation	Ground state Energy (eV)	Energy (Hartree)	Zero point energy (eV)
1	-993,072924685	-623162,6944402	- 992,822791
2	-993.072924692	-623162,6944370	- 992,822791
3	- 993,072924694	-623162,6944376	- 992,822791
4	- 993,073025510	-623162,7577006	- 992,822905
5	- 993,073025507	-623162,7576994	- 992,822905
6	- 993,073025502	-623162,7576962	- 992,822905
7	- 993,072003371	-623162,1162987	- 992,821902
8	- 993,072003398	-623162,1163163	- 992,821902
9	- 993,072003382	-623162,1163056	- 992,821902
10	-993.072924692	-623162,6944370	- 992,822791
11	- 993,071997796	-623162,1128010	- 992,821932
12	- 993,071997797	-623162,1128016	- 992,821932

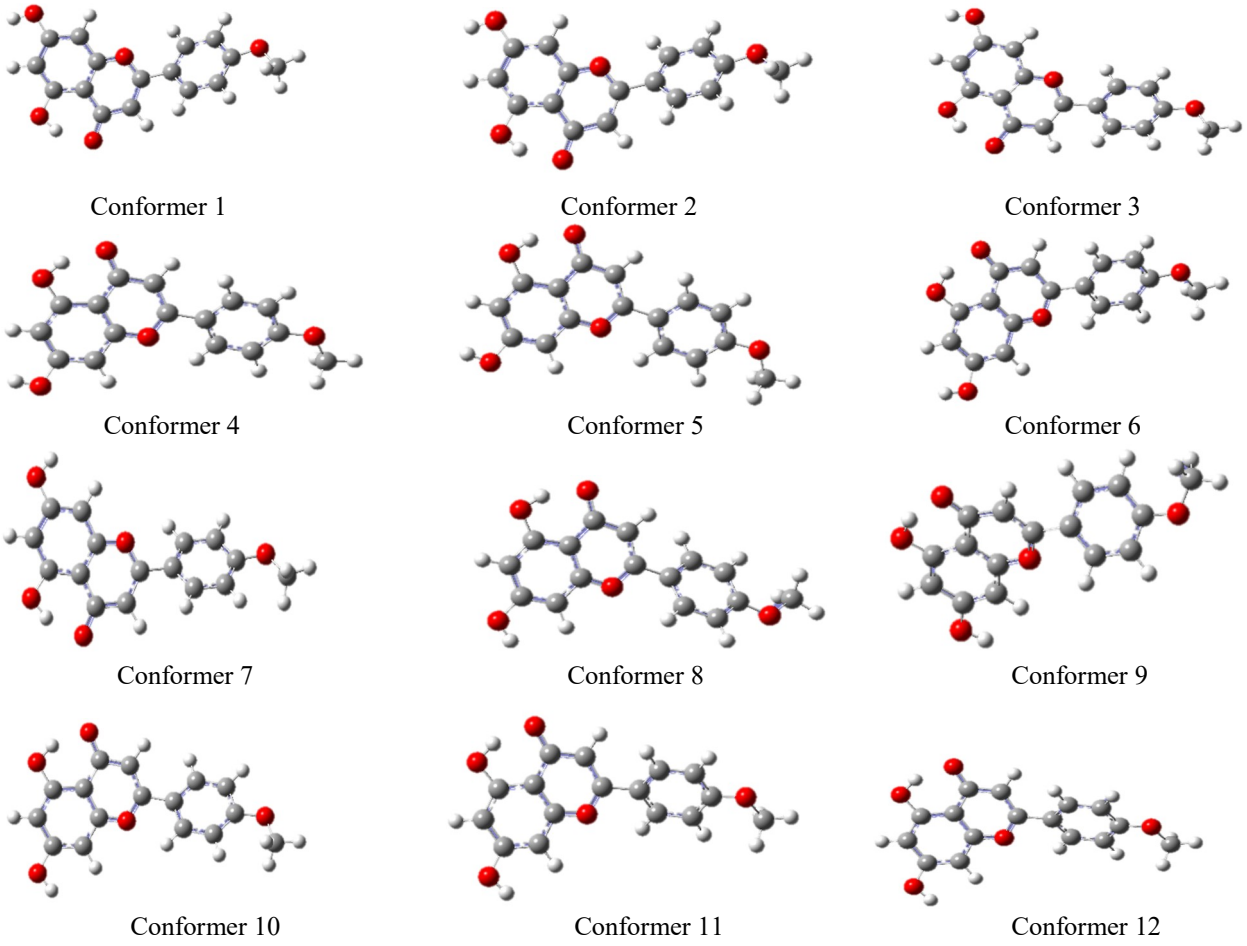

Fig. 3 Stable conformers of acacetin.

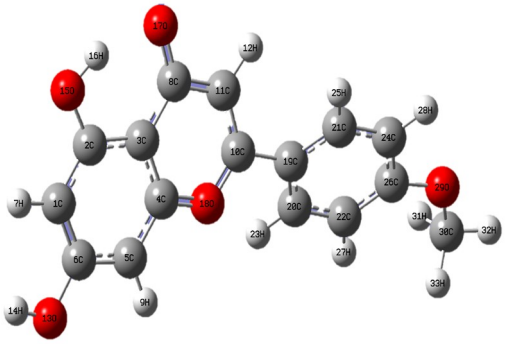

Fig. 4 Molecular structure and atom numbering scheme adopted in this study for acacetin.

The molecular structure with atom numbering scheme for conformer is given in Fig. 4.

In all cases, the trans orientations of the hydroxyl groups given in Fig. 3 are preferred. The main reason of the energy distribution seems to be acacetin orientation relative to the nearest hydroxyl group. Ground state energies, zero point corrected energies (E_{elect} + ZPE), relative energies of conformers were presented in Table 1. From the calculated energies of twelve conformers, given in Table 1, the conformer 4 is the most stable. Zero point corrections have not caused any important changes in the stability order.

4.2. Molecular Geometry

Optimized molecular structure of acacetin is given in Figure 4. We have not found experimental data and the calculation results on molecular structure of acacetin in the literature. That's why the molecular structure of conformer 4 of acacetin molecule was compared with X-Ray data of much the same related molecule like flavone in Table 2 [13].

4.3. Vibrational Analysis

Acacetin molecule has 33 atoms and 93 normal modes of vibrations. All of them are active in the Infrared and Raman spectra. Some of the calculated harmonic vibrational wavenumbers are higher than the experimental ones, because of the anharmonicity of the incomplete treatment of electron correlation and of the use of finite one-particle basis set [12]. The harmonic frequencies were calculated by B3LYP/cc-pVDZ and B3LYP/cc-pVTZ level of theory and then scaled respectively by 0,970 and 0,965 [14]. Scale factors were used to fit the calculated wavenumbers with those of the observed ones. The 93 normal modes of the acacetin molecule have been assigned as per the detailed motion of the individual atoms. Acacetin molecule pertain C_1 symmetry group.

Experimentally and theoretically results of harmonic vibrational frequencies and their correlations were collected in Table 3. From the calculations, the computed values are in good agreement with the observed values. The vibrational bands assignments have been made by using the animation option of Gauss View 5.0.8 graphical interface for Gaussian programs [15] along with available related molecules and also by means of TEDs using the SQM program [16]. IR absorption intensities of acacetin are consistent with the PED results [17].

The heteroaromatic structure indicates that the presence of the C–H stretching vibration in the range 3000–3100 cm^{-1} which is the characteristic region for three C–H stretching vibration [18]. Also, in aromatic compounds, in-plane C–H bending vibrations observe in the range of 1300–1000 cm^{-1} and the C–H out of plane bending vibrations in the range of 1000–750 cm^{-1} [9].

These fundamental C–H bands in acacetin molecule are observed experimentally at 3061 (υ_{85}), 3082 (υ_{86}) and 3142 (υ_{92}) cm^{-1} as medium strong band in Infrared spectra and 3015 and 3077 cm^{-1} as medium strong in Raman spectra. The computed wavenumbers are assigned in the range of 3144–3051 cm^{-1} in Infrared spectra and in the range of 3116–3042 cm^{-1} in Raman spectra. The C–H in-plane bending vibrations of acacetin molecule are observed at 1119–1236 cm^{-1} in the region (FT-IR spectra) and 1170–1237 cm^{-1} in the region (FT-Raman spectra). These in-plane bending vibrations are calculated at 1130–1256 cm^{-1} in the region (B3LYP–cc-pVDZ basis set) and 1130–1256 cm^{-1} in the region (B3LYP–cc-pVTZ basis set). Out-of-plane C–H bending vibrations are observed at 769 cm^{-1} , 851 cm^{-1}, 868 cm^{-1}, 906 cm^{-1} and 925 cm^{-1} for flavone molecule [9]. These vibrations for acacetin molecule are observed the same region. All these theoretical calculations of the C–H vibrations conform to experimental values.

Table.2 Optimized geometric parameters of acacetin

Theoretical(B3LYP)				Theoretical(B3LYP)			
Parameters	cc-PVDZ	cc-PVTZ	X – Ray [13]	Parameters	cc-PVDZ	cc-PVTZ	X – Ray [13]
Bond lengths (Aº)				Bond Angles (º)			
C_1-C_2	1.398	1.389	1.374	C_3-C_4-O_{18}	120.5	120.5	122.3
C_1-C_6	1.403	1.395	1,397	C_5-C_4-O_{18}	116.9	116.8	115.9
C_1-H_7	1.092	1.082		C_4-C_5-C_6	117.7	117.7	
C_2-C_3	1.425	1.418	1.405	C_4-C_5-H_9	121.5	121.4	118.4
C_2-O_{15}	1.335	1.335		C_6-C_5-H_9	120.8	120.9	
C_3-C_4	1.406	1.399	1.393	C_1-C_6-C_5	121.8	121.8	120.9
C_3-C_8	1.454	1.449	1.475	C_1-C_6-O_{13}	121.7	121.5	
C_4-C_5	1.391	1.383	1.395	C_5-C_6-O_{13}	116.5	116.7	
C_4-O_{18}	1.373	1.368	1.374	C_3-C_8-C_{11}	115.1	115.2	114.1
C_5-C_6	1.403	1.393	1.379	C_3-C_8-O_{17}	122.1	122.1	122.3
C_5-H_9	1.089	1.079		C_{11}-C_8-O_{17}	122.9	122.7	123.5
C_6-O_{13}	1.359	1.359		C_{11}-C_{10}-O_{18}	121.5	121.4	122.2
C_8-C_{11}	1.449	1.442	1.448	C_{11}-C_{10}-C_{19}	126.4	126.2	125.8
C_8-O_{17}	1.253	1.247	1.232	O_{18}-C_{10}-C_{19}	112.1	112.4	111.9
C_{10}-C_{11}	1.365	1.355	1.354	C_8-C_{11}-C_{10}	121.7	121.7	122.4
C_{10}-O_{18}	1.365	1.360	1.367	C_8-C_{11}-H_{12}	117.3	117.6	
C_{10}-C_{19}	1.472	1.467	1.475	C_{10}-C_{11}-H_{12}	121.0	120.7	
C_{11}-H_{12}	1.088	1.078		C_6-O_{13}-H_{14}	108.8	109.5	
O_{13}-H_{14}	0.970	0.963		C_2-O_{15}-H_{16}	105.4	106.2	
O_{15}-H_{16}	1.007	0.997		C_4-O_{18}-C_{10}	120.8	120.9	119.1
H_{16}-O_{17}	1.646	1.673		C_{10}-C_{19}-C_{20}	120.8	120.9	121.1
C_{19}-C_{20}	1.405	1.397	1.400	C_{10}-C_{19}-C_{21}	121.4	121.2	119.3
C_{19}-C_{21}	1.412	1.404	1.399	C_{20}-C_{19}-C_{21}	117.8	117.9	119.4
C_{20}-C_{22}	1.396	1.388	1.391	C_{19}-C_{20}-C_{22}	121.6	121.5	120.0
C_{20}-H_{23}	1.089	1.079		C_{19}-C_{20}-H_{23}	119.3	119.5	
C_{21}-C_{24}	1.385	1.377	1.385	C_{22}-C_{20}-H_{23}	119.1	119.0	
C_{21}-H_{25}	1.090	1.080		C_{19}-C_{21}-C_{24}	121.1	121.2	119.6
C_{22}-C_{26}	1.402	1.395	1.393	C_{19}-C_{21}-H_{25}	120.4	120.1	
C_{22}-H_{27}	1.089	1.079		C_{24}-C_{21}-H_{25}	118.5	118.7	
C_{24}-C_{26}	1.408	1.400	1.380	C_{20}-C_{22}-C_{26}	119.8	119.8	120.1
C_{24}-H_{28}	1.091	1.081		C_{20}-C_{22}-H_{27}	119.1	119.2	
C_{26}-O_{29}	1.357	1.355		C_{26}-C_{22}-H_{27}	121.1	121.0	
O_{29}-C_{30}	1.422	1.421		C_{21}-C_{24}-C_{26}	120.4	120.3	121.2
C_{30}-H_{31}	1.104	1.093		C_{21}-C_{24}-H_{28}	121.2	121.1	
C_{30}-H_{32}	1.097	1.086		C_{26}-C_{24}-H_{28}	118.4	118.6	
C_{30}-H_{33}	1.104	1.093		C_{22}-C_{26}-C_{24}	119.2	119.3	119.5
Bond Angles (º)				C_{22}-C_{26}-O_{29}	125.0	124.7	
C_2-C_1-C_6	119.8	119.7	120.1	C_{24}-C_{26}-O_{29}	115.7	115.9	
C_2-C_1-H_7	118.9	119.1		C_{26}-O_{29}-C_{30}	118.5	118.8	
C_6-C_1-H_7	121.4	121.2		O_{29}-C_{30}-H_{31}	111.6	111.3	

C_1-C_2-C_3	119.7	119.9	120.2	O_{29}-C_{30}-H_{32}	105.9	105.9	
C_1-C_2-O_{15}	120.3	120.0		O_{29}-C_{30}-H_{33}	111.6	111.3	
C_3-C_2-O_{15}	120.0	120.1		H_{31}-C_{30}-H_{32}	109.3	109.4	
C_2-C_3-C_4	118.5	118.2	118.5	H_{31}-C_{30}-H_{33}	109.2	109.5	
C_2-C_3-C_8	121.1	121.5	121.8	H_{32}-C_{30}-H_{33}	109.3	109.4	
C_4-C_3-C_8	120.4	120.2	119.6				
C_3-C_4-C_5	122.6	122.7	121.6				

DihedralAngles(°)			DihedralAngles(°)		
C_6-C_1-C_2-C_3	0.0008	0.0336			
C_6-C_1-C_2-O_{15}	179.99	179.94	C_{10}-C_{19}-C_{20}-C_{22}	179.99	179.10
H_7-C_1-C_2-C_3	179.99	179.96	C_{10}-C_{19}-C_{20}-H_{23}	0.0032	0.4459
H_7-C_1-C_2-O_{15}	0.0005	0.0727	C_{21}-C_{19}-C_{20}-C_{22}	0.0003	0.6199
C_2-C_1-C_6-C_5	0.0004	0.0096	C_{21}-C_{19}-C_{20}-H_{23}	179.99	179.84
C_2-C_1-C_6-O_{13}	179.99	179.97	C_{10}-C_{19}-C_{21}-C_{24}	179.99	179.23
H_7-C_1-C_6-C_5	180.00	179.99	C_{10}-C_{19}-O_{21}-H_{25}	0.0013	1.8553
H_7-C_1-C_6-O_{13}	0.0002	0.0183	C_{20}-C_{19}-C_{21}-C_{24}	0.0010	0.4824
C_1-C_2-C_3-C_4	0.0014	0.0881	C_{20}-C_{19}-C_{21}-H_{25}	179.99	178.43
C_1-C_2-C_3-C_8	179.99	179.77	C_{19}-C_{20}-C_{22}-C_{26}	0.0032	0.3120
O_{15}-C_2-C_3-C_4	179.99	179.88	C_{19}-C_{20}-C_{22}-H_{27}	179.99	179.63
O_{15}-C_2-C_3-C_8	0.0023	0.2034	H_{23}-C_{20}-C_{22}-C_{26}	17999	179.86
C_1-C_2-O_{15}-H_{16}	179.99	179.85	H_{23}-C_{20}-C_{22}-H_{27}	0.0035	0.0894
C_3-C_2-O_{15}-H_{16}	0.0021	0.1162	C_{19}-C_{21}-C_{24}-C_{26}	0.0006	0.0393
C_2-C_3-C_4-C_5	0.0009	0.1047	C_{19}-C_{21}-C_{24}-H_{28}	179.99	179.56
C_2-C_3-C_4-O_{18}	179.99	179.83	H_{25}-C_{21}-C_{24}-C_{26}	179.99	178.89
C_8-C_3-C_4-C_5	179.99	179.79	H_{25}-C_{21}-C_{24}-H_{28}	0.0001	0.6284
C_8-C_3-C_4-O_{18}	0.0018	0.4818	C_{20}-C_{22}-C_{26}-C_{24}	0.0047	0.1481
C_2-C_3-C_8-C_{11}	179.99	179.48	C_{20}-C_{22}-C_{26}-O_{29}	179.99	179.89
C_2-C_3-C_8-O_{17}	0.0002	0.1065	H_{27}-C_{22}-C_{26}-C_{24}	179.99	179.91
C_4-C_3-C_8-C_{11}	0.0008	0.1931	H_{27}-C_{22}-C_{26}-O_{29}	0.0009	0.1698
C_4-C_3-C_8-O_{17}	179.99	179.78	C_{21}-C_{24}-C_{26}-C_{22}	0.0034	0.2823
C_3-C_4-C_5-C_6	0.0003	0.0626	C_{21}-C_{24}-C_{26}-O_{29}	179.99	179.96
C_3-C_4-C_5-H_9	179.99	179.75	H_{28}-C_{24}-C_{26}-C_{22}	179.99	179.25
O_{18}-C_4-C_5-C_6	179.99	179.80	H_{28}-C_{24}-C_{26}-O_{29}	0.0039	0.5147
O_{18}-C_4-C_5-H_9	0.0004	0.0087	C_{22}-C_{26}-O_{29}-C_{30}	0.0484	0.0141
C_3-C_4-O_{18}-C_{10}	0.0031	0.5999	C_{24}-C_{26}-O_{29}-C_{30}	179.96	179.73
C_5-C_4-O_{18}-C_{10}	179.99	179.65	C_{26}-O_{29}-C_{30}-H_{31}	61.287	61.241
C_4-C_5-C_6-C_1	0.0010	0.0038	C_{26}-O_{29}-C_{30}-H_{32}	179.95	179.99
C_4-C_5-C_6-O_{13}	179.99	179.99	C_{26}-O_{29}-C_{30}-H_{33}	61.172	61.224
H_9-C_5-C_6-C_1	179.99	179.81	C_{10}-C_{19}-C_{20}-C_{22}	179.99	179.10
H_9-C_5-C_6-O_{13}	0.0002	0.1741	C_{10}-C_{19}-C_{20}-H_{23}	0.0032	0.4459
C_1-C_6-O_{13}-H_{14}	0.0026	0.0306	C_{21}-C_{19}-C_{20}-C_{22}	0.0003	0.6199
C_5-C_6-O_{13}-H_{14}	179.99	179.95	C_{21}-C_{19}-C_{20}-H_{23}	179.99	179.84
C_3-C_8-C_{11}-C_{10}	0.0012	0.7936	C_{10}-C_{19}-C_{21}-C_{24}	179.99	179.23
C_3-C_8-C_{11}-H_{12}	179.99	178.23	C_{10}-C_{19}-O_{21}-H_{25}	0.0013	1.8553
O_{17}-C_8-C_{11}-C_{10}	179.99	179.62	C_{20}-C_{19}-C_{21}-C_{24}	0.0010	0.4824
O_{17}-C_8-C_{11}-H_{12}	0.0024	1.3530	C_{20}-C_{19}-C_{21}-H_{25}	179.99	178.43

O_{18}-C_{10}-C_{11}-C_8	0.0025	0.7290	C_{19}-C_{20}-C_{22}-C_{26}	0.0032	0.3120
C_{18}-C_{10}-C_{11}-H_{12}	179.99	178.27	C_{19}-C_{20}-C_{22}-H_{27}	179.99	179.63
C_{19}-C_{10}-C_{11}-C_8	179.99	179.90	H_{23}-C_{20}-C_{22}-C_{26}	179.99	179.86
C_{19}-C_{10}-C_{11}-H_{12}	0.0047	1.1098	H_{23}-C_{20}-C_{22}-H_{27}	0.0035	0.0894
C_{11}-C_{10}-O_{18}-C_4	0.0034	0.0066	C_{19}-C_{21}-C_{24}-C_{26}	0.0006	0.0393
C_{19}-C_{10}-O_{18}-C_4	179.99	179.46	C_{19}-C_{21}-C_{24}-H_{28}	179.99	179.56
C_{11}-C_{10}-C_{19}-C_{20}	179.98	165.17	H_{25}-C_{21}-C_{24}-C_{26}	179.99	178.89
C_{11}-C_{10}-C_{19}-C_{21}	0.0217	14.539	H_{25}-C_{21}-C_{24}-H_{28}	0.0001	0.6284
O_{18}-C_{10}-C_{19}-C_{20}	0.0271	14.256			
O_{18}-C_{10}-C_{19}-C_{21}	179.97	166.04			

The most intensive peak for flavone molecule is C=O stretching and is observed at 1646 cm^{-1} in Infrared and 1633 cm^{-1} in Raman [9]. This peak is observed at 1581 cm^{-1} in Infrared spectra (1577 cm^{-1} in Raman spectra), is calculated at 1595cm^{-1} for B3LYP–cc-pVDZ basis set and 1577cm^{-1} for B3LYP–cc-pVTZ basis set in our studies.

The O–H group vibrations are likely to be the most sensitive to the environment, therefore they show pronounced shifts in the spectra of the hydrogen-bonded species [12]. The O–H stretching vibrations were calculated at 2963 cm^{-1}–2963 $cm^{-1}$and 3663cm^{-1}–3680 cm^{-1} in B3LYP–cc-pVDZ and cc-pVTZ basis sets in FT-IR spectrum, respectively.

The C–C stretching vibrations in aromatic compounds are seen in the region of 1430–1650 cm^{-1}. The C–C ring stretching vibrations for all rings assigned to 1606 cm^{-1} in the flavone [9]. This stretching vibration is observed at 1605 cm^{-1} in the Infrared spectra (1608 cm^{-1} in the Raman spectra) and is calculated 1610 cm^{-1} for B3LYP–cc-pVDZ level of theory and 1591 cm^{-1} in B3LYP–cc-pVTZ level of theory, respectively.

A comparison of these bands with experimental data predicts that there are negative deviations indeed the presence of strong intermolecular hydrogen bonding.

4.4 Molecular Electrostatic Potential (Mesp)

The electron potential surface molecules of acacetin molecules, shapes, sizes and electrostatic potential values of this molecule were plotted using DFT model. In addition, a three-dimensional surface potential map of electron density of the molecule was drawn [19]. The two dimensional and three dimensional MESP maps of acacetin molecule were visualized in Figure 5. There is an excess of electrons in the red zone in colorful map of the molecule. That is, these red zones are negatively charged. The regions having the negative potential are over oxygen atoms. In other areas there is a lack of electrons and positively charged. While red color zones indicate the strongest pushing, blue color zones indicate the strongest pulling. The MESP map of acacetin molecule clearly shows that of electron-rich oxygen atoms.

4.5. Homo-Lumo Analysis

The highest occupied molecular orbital (HOMO) and the lowest empty molecular orbital (LUMO) are very important parameters for the quantum chemistry. We identify with this way of interacting with other molecules of a molecule. They are called the frontier orbitals. HOMO, which can be thinking the outermost orbital including electrons, tends to give these electrons such as an electron donor. On the other hand, LUMO can be thinking the intermost orbital including free places to accept electrons [20].

Because of the interaction between HOMO and LUMO orbital of a structure, transition state of π - π^* type is observed in point of the molecular orbital theory [21]. That's why, while the energy of the HOMO is directly related to the ionization potential, LUMO energy is directly related to the electron affinity [22]. The energy difference of the HOMO-LUMO energy levels is called the energy band gap. This is an important parameter for the stability of the structure. Three-dimensional graphics of HOMO and LUMO for the acacetin molecule is shown in Fig.6. HOMO and LUMO energy levels B3LYP/cc-pVDZ calculated. According to these calculations, the energy band gap of the molecules is 4.0294 eV. Found that the eigen values of HOMO, LUMO and their energy gap reflect the chemical activity of the acacetin molecule. Furthermore, the lower in the HOMO LUMO energy gaps elucidate the eventual charge transfer interactions taking place within acacetin. The highest occupied molecular orbitals were usually localized on all groups.

Table.3 Vibrational assignment of ACACETIN by normal mode analysis based on SQM force field calculations.

Theoretical (B3LYP)								Experimental		TED[c] (%)
cc-PVDZ				cc-PVTZ				Exp. IR	Exp. Raman	
Normal Modes.	Freq[a]	I^b_{IR}	I^b_{Raman}	Freq[a]	Ra [5]	SERS[5]	Gas Phase [6]			
ν_1	11	0,013	0,111	24						$\tau_{CCCC}(34) + \tau_{CCCO}(34) + \tau_{HCCC}(12)$
ν_2	37	0,023	0,043	37						$\tau_{CCCC}(29) + \tau_{CCOC}(19) + \tau_{CCCO}(18) + \tau_{CCCH}(15)$
ν_3	75	0,017	0,154	70						$\delta_{CCC}(36) + \delta_{CCO}(21) + \nu_{CC}(12) + \nu_{OH}(10)$
ν_4	84	0,042	0,082	86					96 vs	$\tau_{CCOC}(26) + \tau_{CCCC}(23) + \tau_{CCCO}(15) + \tau_{COCH}(15)$
ν_5	101	0,020	0,021	102					114 s	$\tau_{CCCC}(33) + \tau_{CCCO}(31) + \tau_{CCOC}(12)$
ν_6	126	0,793	0,070	124					134 m	$\tau_{CCCC}(26) + \tau_{CCOC}(24) + \tau_{CCCO}(17) + \tau_{CCCH}(12) + \tau_{COCH}(11)$
ν_7	171	0,019	0,019	169					165 m	$\tau_{CCCC}(31) + \tau_{CCCO}(30) + \tau_{CCCH}(11) + \tau_{CCOC}(11)$
ν_8	203	0,027	0,138	201						$\delta_{CCC}(24) + \delta_{CCO}(24) + \nu_{CC}(15) + \nu_{OH}(15)$
ν_9	217	0,020	0,012	212						$\tau_{CCCO}(29) + \tau_{CCCC}(20) + \tau_{COCH}(15) + \tau_{CCOC}(10)$
ν_{10}	219	0,212	0,122	218					219 m	$\delta_{CCC}(28) + \delta_{CCO}(24) + \nu_{CC}(16)$
ν_{11}	232	0,031	0,191	226					238 m	$\tau_{COCH}(27) + \tau_{CCCO}(23) + \tau_{CCCC}(22)$
ν_{12}	247	0,006	0,062	246						$\tau_{CCCC}(27) + \tau_{CCCO}(20) + \tau_{COCH}(18) + \tau_{CCOC}(14)$
ν_{13}	281	0,174	0,069	281						$\tau_{CCCO}(31) + \tau_{CCCC}(30) + \tau_{CCCH}(10)$
ν_{14}	284	2,601	0,211	282	295				294 m	$\delta_{CCO}(23) + \delta_{CCC}(22) + \nu_{OH}(22)$
ν_{15}	336	0,069	0,107	333		346				$\tau_{CCCC}(26) + \tau_{CCCO}(22) + \tau_{CCOC}(13) + \tau_{COCH}(11)$
ν_{16}	345	0,994	0,173	344					337 w	$\nu_{OH}(31) + \delta_{CCO}(24) + \delta_{CCC}(20) + \nu_{CC}(10)$
ν_{17}	363	0,802	0,170	362						$\delta_{CCC}(27) + \delta_{CCO}(21) + \nu_{CC}(15) + \nu_{OH}(14)$
ν_{18}	398	13,621	0,217	383						$\tau_{CCOH}(63) + \tau_{CCCH}(10)$
ν_{19}	410	0,001	0,007	411				410 w,sh		$\tau_{CCCC}(43) + \tau_{CCCH}(30) + \tau_{CCCO}(12)$
ν_{20}	416	0,758	0,347	414				422 w	435 m	$\delta_{CCC}(31) + \delta_{CCO}(19) + \nu_{OH}(13) + \nu_{CC}(12)$
ν_{21}	446	0,234	0,181	417		449		461 m	458 w	$\delta_{CCC}(26) + \delta_{CCO}(21) + \delta_{CCH}(12) + \nu_{CC}(10)$
ν_{22}	498	0,342	0,595	497						$\delta_{CCC}(38) + \delta_{CCO}(21) + \delta_{CCH}(11)$
ν_{23}	505	0,396	0,090	502	501			503 s		$\delta_{CCC}(30) + \delta_{CCO}(28) + \delta_{CCH}(12)$

ν_{24}	506	0,956	0,032	508	511			521 s	514 w	τ_{CCCH} (33) + τ_{CCCC}(32) + τ_{CCCO} (12)
ν_{25}	552	2,526	0,236	552		520		557 vs	560 w	δ_{CCC}(34) + δ_{CCO}(28) +δ_{CCH}(15)
ν_{26}	569	6,797	1,624	569				580 s	583 vs	δ_{CCC}(25) + δ_{CCO}(19) +δ_{CCH}(15) +ν_{CC} (12) + ν_{CO} (11)
ν_{27}	608	0,158	0,054	605				606 w		τ_{CCCC}(26) + τ_{CCCO} (24) + τ_{CCCH} (19)
ν_{28}	621	2,820	1,348	619	621	614				δ_{CCC}(28) + δ_{CCO}(25) +δ_{CCH}(14) +ν_{CC} (12)
ν_{29}	628	0,363	1,000	624					629 w,sh	δ_{CCC}(34) +δ_{CCH}(25) + δ_{CCO}(11) +ν_{CC} (14)
ν_{30}	629	0,631	0,046	629						τ_{CCCC}(25) + τ_{CCCO} (20)+τ_{CCCH} (20) + τ_{OCCH}(14)
ν_{31}	650	0,130	0,065	650	652			636 s	641 s	τ_{CCCC}(35) + τ_{CCCH} (24) + τ_{CCCO} (17)
ν_{32}	661	0,928	0,117	662				660 m,sh	659 w	τ_{CCCC}(41) + τ_{CCCH} (20) + τ_{CCCO} (14)
ν_{33}	668	0,420	0,661	668	675	680		684 s	688 m	δ_{CCC}(27) +δ_{CCO}(19) +ν_{CC} (15)
ν_{34}	726	0,488	0,394	722				703 s	709 vw	δ_{CCO}(24) + δ_{CCC}(23) +ν_{CC} (20) + δ_{CCH}(16)
ν_{35}	734	0,079	0,165	730				712 w,sh	732 vw	τ_{CCCC}(32) + τ_{CCCH} (27) + τ_{CCCO} (14)
ν_{36}	755	0,882	0,002	761		746	755	757 vs	747 m	τ_{CCCH} (23) + τ_{CCCC}(21) + τ_{CCCO} (21)
ν_{37}	789	1,032	2,251	786						δ_{CCC}(30) +ν_{CC} (18) + δ_{CCH}(14) + ν_{CO} (11)
ν_{38}	792	3,570	0,069	798						τ_{OCCH} (31) + τ_{CCCC}(17) + τ_{CCCH} (13)
ν_{39}	801	0,077	0,187	800				783 s	797 s	τ_{CCCH} (58) + τ_{OCCH} (20)
ν_{40}	806	3,562	0,190	810				806 s		τ_{CCCH} (33) + τ_{OCCH} (28) + τ_{CCCC}(19)
ν_{41}	834	7,613	0,196	831		838		823 vs		τ_{CCCH} (38) + τ_{OCCH} (21) + τ_{CCCC}(12)
ν_{42}	843	0,002	0,119	843	856			839 s	840 w	τ_{CCCH} (36) + τ_{OCCH} (21) + τ_{CCCC}(20)
ν_{43}	890	1,629	0,964	879					865 w	ν_{CC} (24) + δ_{CCC}(22) + δ_{CCO}(20) +δ_{CCH}(14)
ν_{44}	898	12,694	0,067	889				906 m	909 m	τ_{CCOH} (46) + τ_{CCCO} (17) + τ_{CCCC}(16)
ν_{45}	949	0,0001	0,159	943		929				τ_{CCCH} (44) + τ_{HCCH} (19) + τ_{CCCC}(18)
ν_{46}	952	0,005	0,022	952						τ_{CCCH} (48) + τ_{HCCH} (21) + τ_{CCCC}(12)
ν_{47}	963	0,380	0,371	960				959 w,sh	944 w	δ_{CCC}(26) +ν_{CC} (22)+δ_{CCH}(21) + ν_{CO} (12) + δ_{CCO}(10)
ν_{48}	990	0,500	0,087	993					981 w	δ_{CCC}(31) +δ_{CCH}(31) +ν_{CC} (20)
ν_{49}	1010	1,952	0,357	1011	1002	1005		1009 m		δ_{CCH}(37) +ν_{CC} (19)+δ_{CCC}(13) + ν_{CO} (12)
ν_{50}	1037	11,580	0,183	1023	1013			1032 s	1029 w	ν_{CO} (23) + δ_{CCH}(22) +δ_{CCC}(15) +ν_{CC} (13)
ν_{51}	1088	7,241	0,293	1080	1048			1063 w,sh		δ_{CCC}(22) + δ_{CCO}(17) +ν_{CC} (16)+ν_{CO} (16) + δ_{CCH}(12)
ν_{52}	1094	3,773	1,744	1094		1098		1097 m		δ_{CCH}(42) +ν_{CC} (19) + δ_{CCC}(17) + δ_{CCO}(11)

ν_{53}	1105	1,293	0,381	1108	1100					$\delta_{CCH}(46) + \nu_{CC}(16) + \delta_{CCC}(13)$
ν_{54}	1123	0,115	0,145	1132					1125 w	$\delta_{OCH}(40) + \tau_{COCH}(28) + \delta_{HCH}(13) + \tau_{CCOC}(10)$
ν_{55}	1130	33,177	0,727	1133	1143			1119 m		$\delta_{CCH}(53) + \nu_{CC}(13) + \nu_{CO}(12)$
ν_{56}	1157	22,984	11,523	1161				1145 s,sh		$\delta_{CCH}(62) + \nu_{CC}(13)$
ν_{57}	1160	0,390	0,226	1162	1162			1165 vs	1170 w	$\delta_{OCH}(31) + \tau_{COCH}(18) + \delta_{CCH}(18) + \delta_{HCH}(11)$
ν_{58}	1163	5,694	0,404	1166		1170		1186 vs	1187 s	$\delta_{CCH}(37) + \nu_{CO}(16) + \nu_{CC}(12) + \delta_{CCC}(11)$
ν_{59}	1218	17,560	15,641	1210	1195			1211 m,sh		$\delta_{CCH}(35) + \nu_{CC}(20) + \delta_{CCC}(12) + \nu_{CO}(10) + \delta_{COH}(10)$
ν_{60}	1229	14,190	14,459	1226	1235			1217 m,sh		$\delta_{CCH}(37) + \nu_{CC}(19) + \nu_{CO}(12) + \delta_{CCC}(10)$
ν_{61}	1256	22,256	3,856	1244		1244		1236 vs	1237 s	$\delta_{CCH}(26) + \nu_{CC}(20) + \delta_{CCC}(16) + \nu_{CO}(12)$
ν_{62}	1269	25,458	7,989	1253	1270	1256		1277 s	1272 m	$\nu_{CC}(24) + \delta_{CCH}(19) + \nu_{CO}(14)$
ν_{63}	1281	2,749	0,068	1282						$\delta_{CCH}(59) + \nu_{CC}(12)$
ν_{64}	1305	48,745	13,139	1297				1298 s	1299 s	$\nu_{CC}(31) + \delta_{CCH}(20) + \delta_{CCO}(11) + \nu_{CO}(10)$
ν_{65}	1324	3,428	2,918	1300				1321 m	1322 s	$\nu_{CC}(36) + \delta_{CCH}(15) + \delta_{CCC}(12)$
ν_{66}	1359	30,299	6,245	1336	1336	1322		1352 m		$\nu_{CC}(29) + \delta_{CCC}(19) + \delta_{CCH}(17) + \nu_{CO}(15) + \delta_{CCO}(10)$
ν_{67}	1391	11,267	5,347	1368	1377	1359		1367 s	1378 m	$\nu_{CC}(35) + \delta_{CCH}(16) + \delta_{CCC}(12) + \delta_{CCO}(12)$
ν_{68}	1413	17,950	8,768	1405		1403		1403 w,sh		$\delta_{CCH}(35) + \nu_{CC}(16) + \delta_{CCC}(12) + \delta_{HCH}(10)$
ν_{69}	1416	1,743	0,421	1413						$\delta_{HCH}(29) + \delta_{OCH}(29) + \delta_{CCH}(19)$
ν_{70}	1419	0,935	1,632	1428						$\delta_{HCH}(47) + \tau_{COCH}(34) + \delta_{OCH}(11)$
ν_{71}	1431	2,498	1,218	1439						$\delta_{HCH}(25) + \tau_{COCH}(13) + \nu_{CC}(11) + \delta_{CCH}(10)$
ν_{72}	1436	3,966	3,690	1444	1452			1429 vs	1443 m	$\nu_{CC}(16) + \delta_{CCH}(14) + \delta_{CCC}(14) + \delta_{HCH}(11)$
ν_{73}	1455	23,544	2,837	1454	1470		1474	1455 m,sh		$\delta_{CCH}(22) + \nu_{CC}(21) + \delta_{CCC}(13) + \nu_{CO}(13) + \delta_{CCO}(13)$
ν_{74}	1498	43,282	0,150	1490			1495	1473 m,sh		$\delta_{CCH}(43) + \nu_{CC}(20)$
ν_{75}	1508	25,583	15,790	1497				1504 s	1515 m	$\delta_{CCH}(31) + \nu_{CC}(21) + \delta_{CCC}(16) + \delta_{CCO}(11)$
ν_{76}	1561	12,899	32,959	1544				1541 s,sh	1523 m	$\nu_{CC}(36) + \delta_{CCH}(29) + \delta_{CCC}(17)$
ν_{77}	1583	9,635	34,517	1563	1570	1556		1560 s	1561 s	$\nu_{CC}(33) + \delta_{CCH}(20) + \delta_{CCC}(16) + \delta_{CCO}(13)$
ν_{78}	1595	3,062	3,088	1577				1581 m	1573 m	$\nu_{CC}(30) + \delta_{CCC}(16) + \delta_{CCO}(13) + \delta_{CCH}(12) + \nu_{CO}(10)$
ν_{79}	1610	100,000	100,000	1591				1605 vs	1608 vs	$\nu_{CC}(31) + \delta_{CCH}(28) + \delta_{CCC}(21)$
ν_{80}	1622	34,472	0,218	1602	1603	1603	1653	1626 m		$\nu_{CC}(28) + \delta_{CCH}(24) + \delta_{CCC}(17)$
ν_{81}	1662	68,375	26,388	1640	1634	1636	1683	1651 s	1650 m	$\nu_{CC}(28) + \delta_{CCC}(16) + \delta_{CCO}(14) + \delta_{CCH}(14)$

ν_{82}	2918	9,450	10,630	2906				2902 w	2927vw	ν_{CH} (88)
ν_{83}	2963	72,321	10,067	2963		2929		2960 w	2963 vw	ν_{OH} (86)
ν_{84}	2985	4,827	4,512	3026			3025	2991 w,sh	2996 vw	ν_{CH} (81)
ν_{85}	3051	2,836	11,709	3042				3061 m,sh	3015 w	ν_{CH} (81)
ν_{86}	3090	1,142	12,547	3067				3082 m	3077 m	ν_{CH} (74)
ν_{87}	3103	0,718	5,027	3077	3075					ν_{CH} (79)
ν_{88}	3118	0,990	3,994	3091						ν_{CH} (80)
ν_{89}	3118	0,651	6,425	3091						ν_{CH} (81)
ν_{90}	3134	0,426	4,222	3105						ν_{CH} (81)
ν_{91}	3134	0,008	4,685	3109						ν_{CH} (72)
ν_{92}	3144	0,315	6,125	3116			3095	3142 m		ν_{CH} (75)
ν_{93}	3663	13,423	13,131	3680						ν_{OH} (91)

vs: very strong, ms: medium strong, s: strong, w: weak, vw: very weak, ν: stretching, t: torsion, γ: out of plane stretching, δ: in plane bending

[a]Obtained from the wavenumbers calculated at 0.970 for cc-pVDZ, 0.965 for cc-pVTZ [14]

[b]Relative absorption intensities and Relative Raman intensities normalized with highest peak absorption equal to 100

[c] Total energy distribution calculated B3LYP/cc-pVDZ level of theory. Only contributions≥ 10% are listed

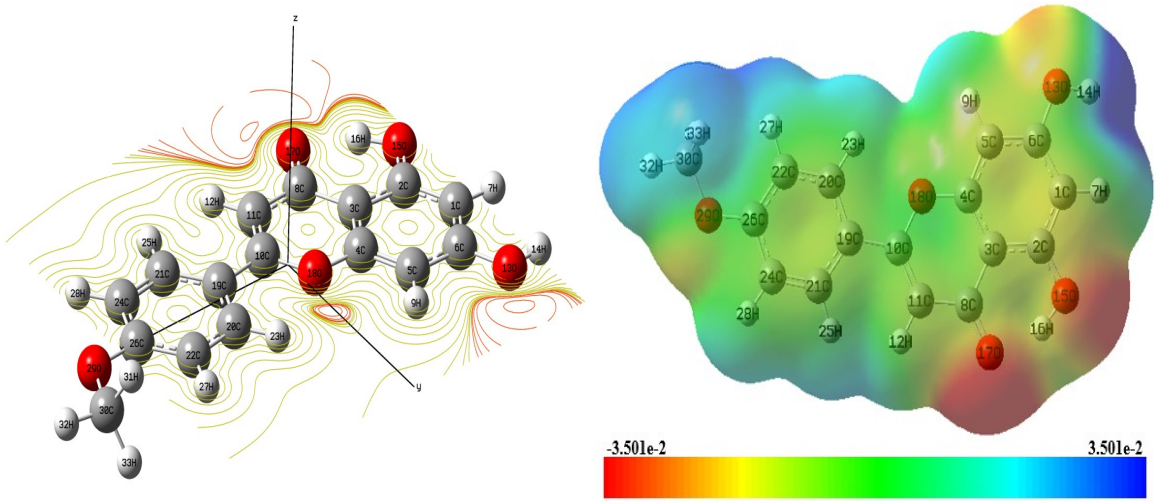

Fig.5 The 2-dimensional and 3-dimensional MESP maps of the acacetin molecule

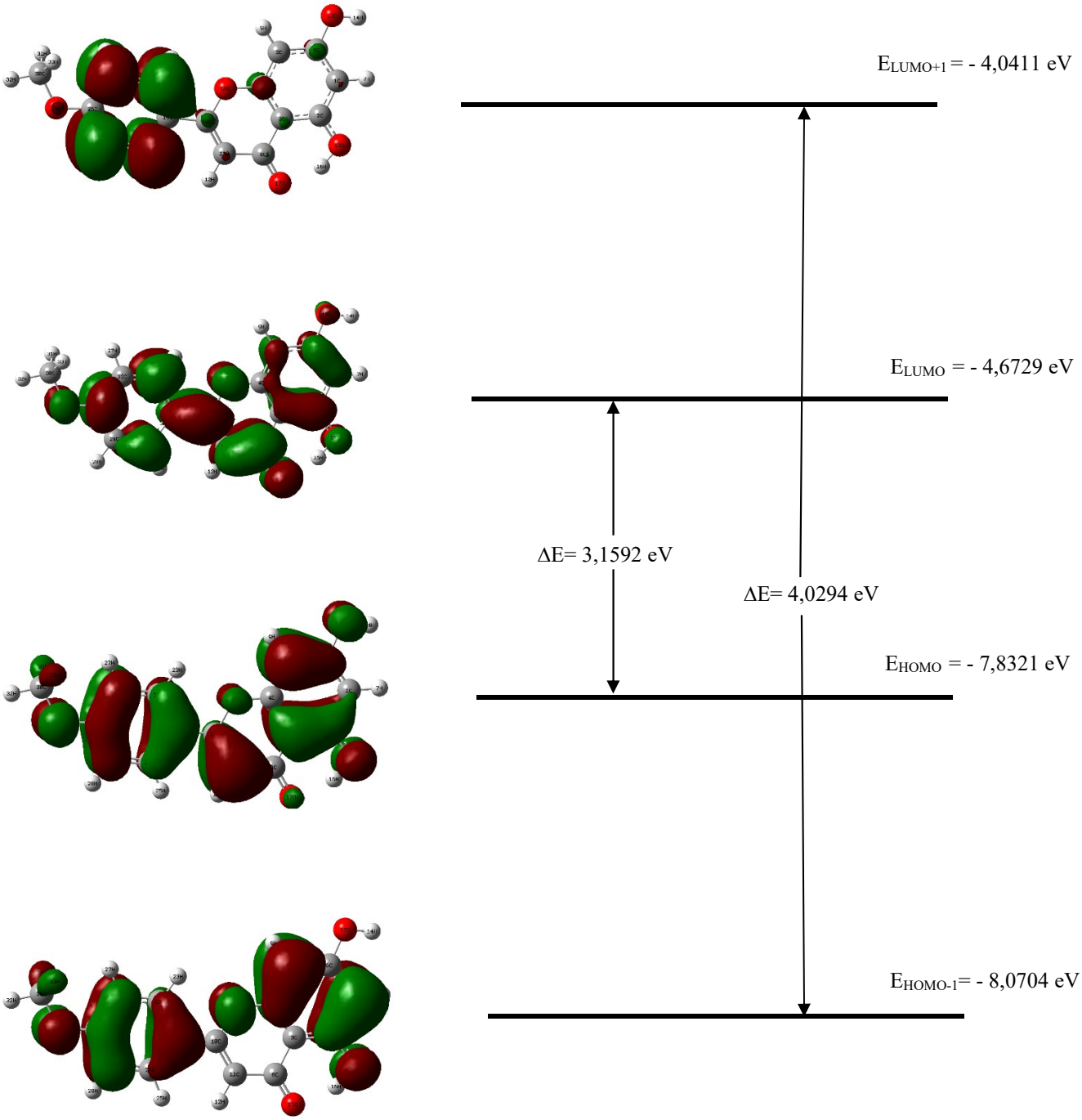

Fig. 6 The atomic compositions of the frontier molecular orbital for acacetin molecule

5. CONCLUSION

We have realized DFT calculations on the title molecule (B3LYP–cc-pVDZ and cc-pVTZ basis sets) and vibrational spectrum (Infrared and Raman spectra) of acacetin molecule. Scale factors were used on account of compare how the calculated wavenumbers were comprised with those of experimental ones. Results are in good agreement with their experimental values. A comparison of these wavenumbers with experimental data predicts that there are negative deviations indeed the presence of strong intermolecular hydrogen bonding. The Infrared and Raman intensities calculated by B3LYP–cc-pVDZ and cc-pVTZ basis sets agree very well with experimental results. Detailed interpretation of the normal nodes has been made on the basis of PED calculations. IR absorption intensities of acacetin are consistent with the PED results. The MESP shows the negative potential sites are on oxygen atoms as well as the positive potential sites are around the hydrogen atoms. The MESP map of acacetin molecule clearly shows that of electron-rich oxygen atoms. HOMO and LUMO energy gap reveals that the energy gap reflects the chemical activity of the molecule. Thus the present investigation provides complete vibrational assignments of the compound. Also, the highest occupied molecular orbitals were usually localized on all groups.

ACKNOWLEDGEMENT

We want to thanks to Prof. Dr. Mustafa KURT for the Gaussian 09W program package.

REFERENCES

[1] P. J. A. Madeira, C. M. Borges and M. H. Florencio, " Electrospray ionization Fourier transform ion cyclotron resonance mass spectrometric and semi-empirical calculations study of five isoflavone aglycones ", Rapid Commun. Mass Spect., v. 24, pp. 3432–3440, 2010.

[2] Y. S. Touil, A. Fellous, D. Scherman and G. G. Chabot, Nutrition and Cancer, "Flavonoid-induced morphological modifications of endothelial cells through microtubule stabilization", v. 61(3), pp. 310–321, 2009.

[3] Shang-Tao Chien, Su-Shun Lin, Cheng-Kun Wang, Yuan-Bin Lee, Kun-Shiang Chen, Yao Fong,Yuan-Wei Shih, "Acacetin inhibits the invasion and migration of human non-small cell lung cancer A549 cellsby suppressing the p38α MAPK signaling pathway", Mol. Cell Biochem. , v. 350, pp. 135–148, 2011.

[4] H. G. Kim, M. S. Ju, S. K. Ha, H. Lee, S. Y. Kim, M. S. Oh, " Acacetin protects dopaminergic cells against 1-methyl-4-phenyl-1, 2, 3, 6-tetrahydropyridine-induced neuroinflammation in vitro and in vivo", Bio. Pharm Bull. , v. 35(8), pp. 1287–1294, 2012.

[5] T. Teslova, C. Corredor, R. Livingstone, T. Spataru, R. L. Birke, J. R. Lombardi, M. V. Canamares and M. Leona, " Raman and surface - enhanced Raman spectra of flavone and several hydroxy derivatives " J. Raman Spect. , v. 38, pp. 802–818 , 2007.

[6] A. Vavra, R. Linder, K. Kleinermanns, "Gas phase infrared spectra of flavone and its derivates ", Chem. Phys. Lett. , v. 463, pp. 349–352 , 2008.

[7] A. Mantas, E. Deretey, F. H. Ferretti, M. Estrada, I. G. Csizmadia, "Ab initio conformational analysis of flavone and related compounds ", J. Mol. Struct., v. 504, pp. 77–103, 2000.

[8] L. Vrielynck, J. P. Cornard, J. C. Merlin and M. F. Lautie, "Semi-empirical and vibrational studies of flavone and some deuterated analogues", Spectrochim. Acta A, v. 50, pp. 2177–2188, 1994.

[9] Y. Erdoğdu, O. Ünsalan and M. T. Güllüoğlu, "Vibrational analysis of flavone ", Turk J. Phys., v. 33, pp. 249–259, 2009.

[10] M.J. Frish et. al., Gaussian 09, Revision A.1, Gaussian Inc. , Wallingford CT, 2009.

[11] H. B. Schlegel, "Optimization of equilibrium geometries and transition structures ", J. Comput. Chem., v. 3, pp. 214–218, 1982.

[12] Ö. Dereli et al. , "Vibrational spectral and quantum chemical investigations of tert-butyl-hydroquinone ", J.Mol.Struct. , v. 1012, pp. 168–176, 2012.

[13] M. P. Waller, D. E. Hibbs, J. Overgaard, J. R. Hanrahanand T. W. Hambley, "Flavone ", Acta Crystallographica Section E, v. 59, pp. 767–768, 2003.

[14] http://cccbdb.nist.gov/vibscalejust.asp

[15] E .Frish, H.P. Hratchian, R.D. Dennington II, T.A. Keith, John Millam, B. Nielsen, A.J. Holder, J. Hiscocks, Gaussian. Inc., GaussViewVersion 5.0.8 , 2009.

[16] G. Rauhut, P. Pulay, "Transferable scaling factors for density functional derived vibrational force fields ", J. Phys. Chem. , v. 99, pp. 3093–3100, 1995.

[17] P. Pulay and F. Török, "Parameter form of the force constant matrix II ", Acta Chimica Acad. Sci. Hung. , v. 47, pp. 273–279 , 1966.

[18] H. Saleem, Y. Erdoğdu, S. Subashchandrabose, Ö. Dereli, V. Thanikachalam and J. Jayabharathi, "Structural, vibrational and hyperpolarizability calculation of (E)-2-(2-hydroxybenzylideneamino)-3-methylbutanoic acid ", Spectrochimica Acta Part A, v. 86, pp. 231–241, 2012.

[19] I. Fleming, "Frontier Orbitals and Organic Chemical Reactions", John Wiley and Sons, New York, 1976.
[20] G. Gece, "The use of quantum chemical methods in corrosion inhibitor studies.", Corrosion Science, v. 50, pp. 2981–2992, 2008.
[21] K. Fukui, "Theory of Orientation and Stereo Selection." Springer-Verlag, Berlin, 1975.
[22] S. Muthu, E. Elamurugu Porchelvi, "FTIR, FT-Raman, NMR, spectra, normal coordinate analysis, NBO, NLO and DFT calculation of N,N-diethyl-4-methyl-piperazine-1-carboxamide molecule", v. 115, pp. 275–286, 2013.